CHAPTER IV

THE SYNERGISTIC EFFECT OF SELECTIVE SEPARATION OF (*S*)-AMLODIPINE FROM PHARMACEUTICAL WASTEWATER VIA A HOLLOW FIBER SUPPORTED LIQUID MEMBRANE

Niti Sunsandee [a], Prakorn Ramakul [b], Nopphawat Thamphiphit [a], Ura Pancharoen [a,*] Natchanun Leepipatpiboon [c,**]

[a] *Department of Chemical Engineering, Faculty of Engineering, Chulalongkorn University, Bangkok 10330, Thailand.*

[b] *Department of Chemical Engineering, Faculty of Engineering and Industrial Technology, Silpakorn University, Nakhon Pathom 73000, Thailand.*

[c] *Chromatography and Separation Research Unit, Department of Chemistry, Faculty of Science, Chulalongkorn University, Patumwan, Bangkok 10330, Thailand.*

This article has been published in Journal: Chemical Engineering Journal. Page: 201–214. Volume: 209. Year: 2012.

4.1 ABSTRACT

A synergistic effect of selective separation of (*S*)-amlodipine using the di(2-ethylhexyl)phosphoric acid (D2EHPA) with the tartaric acid derivatives, *O*,*O*'-dibenzoyl-(2*S*,3*S*)-tartaric acid ((+)-DBTA) was developed for the enantioseparation of racemic amlodipine. The extractants were diluted in 1-decanol with various proportions. The influences of the extractant compositions, the concentrations of amlodipine enantiomers and the extractive equilibrium temperatures were studied. The extraction and recovery of (*S*)-amlodipine from the feed phase in a single-module operation were 84.50% and 80.50%, respectively. The maximum percentage of enantiomeric excess of (*S*)-amlodipine was 70.21%. The aqueous-phase mass-transfer coefficient (k_f) and organic-phase mass-transfer coefficient (k_m) were reported to 4.87×10^{-2} and 2.89×10^{-2} cm/s, respectively. Therefore, the mass transfer-controlling step is the diffusion of (*S*)-amlodipine complex through liquid membrane. The potential application of the synergistic system to separate (*S*)-amlodipine from pharmaceutical wastewaters has also been discussed. The results showed that synergistic extraction technique can be applied for large-scale production of the pure enantiomeric compound.

4.2 INTRODUCTION

Amlodipine is a third-generation dihydropyridine calcium channel blocker prescribed for the management of angina and hypertension [1]. As a racemic mixture, amlodipine contains (*S*)-amlodipine (Figure 4.1(a)) and (*R*)-amlodipine (Figure 4.1(b)), but only (*S*)-amlodipine as the active moiety possesses therapeutic activity [2]. Based on pharmacologic research [3], it remains uncertain if (*S*)-amlodipine alone has similar efficacy and fewer associated adverse events compared with the racemic mixtures [4]. (*S*)-amlodipine exhibits vasodilating properties [5]. Its (*R*)-amlodipine is inactive and thought to be responsible for pedal edema observed with racemic amlodipine [6]. In addition to longer duration of action of (*S*)-amlodipine, it reduces the chances of reflex tachycardia and its clearance is subjected to much less inter-subject variation than (*R*)-amlodipine [7].

Many researchers were studied about the separation of (*S*)-amlodipine. The conventional method e.g. crystallization [8], kinetic resolution [9], chromatography [10] and capillary electrophoresis [11] etc. accelerate researches about chiral compounds, but there still exist some defects for most racemic compounds. Diastereomeric crystallization is the most used method for resolution of racemic mixtures [12]. However, this technique usually requires many steps, increasing the complexity of the process and leading to a considerable loss of product. The application of kinetic resolution is limited due to lengthy development time and availability of enantiomerically differentiating materials [13]. Preparative chromatography and capillary electrophoresis are not suitable for production of large quantities of chiral substances since it employs a substantial amount of solvent and requires significant capital investment [14].

Hollow fiber supported liquid membrane (HFSLM) is renowned as an effective simultaneous process to extract and recover compound from a very dilute solution of interested component in the feed by a single-unit operation [15]. HFSLM follows certain rules for the choice of separation system and has a large application range [16-19]. As a potential large-scale production technique, HFSLM has attracted a lot of researchers to make great efforts in recent years [20-23].

Over recent years, attention has increased in the use of HFSLM as selective separation barriers [24]. In the pores of a microporous support, the solution of optically pure organic compound is immobilized, which selectively transfers preferentially one of the enantiomers of the solute between the two compartment solutions of the membrane [25]. HFSLM draws considerable interest due to its industrial applications [26]. Some other advantages of the hollow fiber contactor over traditional separation techniques include lower capital and operating costs [27], lower energy consumption [28], less solvent used and high selectivity [29]. Moreover, the membrane reactor process is an interested technology in wastewater treatment. The membrane technology has attracted the attention of many researchers for industrial water and wastewater treatments. Yeung's team was one team of the potential group researchers [30-32]. Their work successfully demonstrated the use of inorganic membranes for water and wastewater treatments [30]. The membrane was tested for water pervaporation and ozone water treatment [31]. Their work shows that the membrane contactor is possible to achieve enhanced ozone water treatment from a

compact membrane reactor unit that uses the combined function of membrane as distributor, contactor and separator [31]. Yeung's team is currently investigating a new ozone membrane reactor for treatment of recalcitrant organic pollutants in water [31-33]. Membrane and membrane processes represent important environmental technology for pollution remediation, clean fuel production, green chemical synthesis and wastewater treatment process [33]. The novel membrane reactor is a potential process in industry for the water and wastewater treatments. As mentioned above, HFSLM process is one of very challenging membrane processes for the pharmaceutical wastewater treatment.

In this work, the novel synergistic enantioseparation of (*S*)-amlodipine from racemic amlodipine has been investigated. A chiral selective extractant, *O,O'*--dibenzoyl-(2*S*,3*S*)-tartaric acid ((+)-DBTA) (Figure 4.1(c)) and achiral extractant, di(2-ethylhexyl)phosphoric acid (D2EHPA) (Figure 4.1(d)), were mixed together for their synergistic effect.

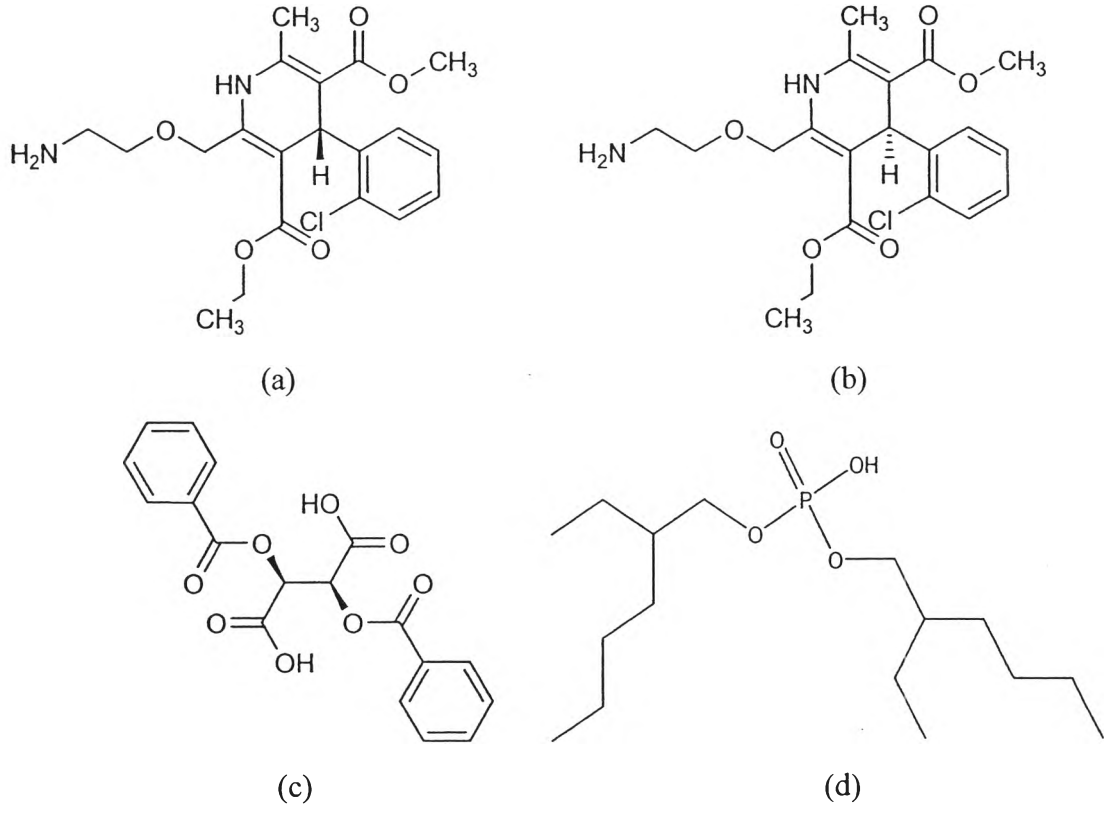

Figure 4.1 Structures of (a) (*S*)-amlodipine, (b) (*R*)-amlodipine (c) *O,O'*--dibenzoyl-(2*S*, 3*S*)-tartaric acid, (d) di(2-ethylhexyl)phosphoric acid (D2EHPA)

4.3 THEORY

4.3.1 Transport mechanism and enantioseparation of (*S*)-amlodipine

A liquid membrane consists of an organic solution of chiral selector as the extractant, which is held in polymeric micropores by capillary action [34]. The supported liquid membrane lies between the aqueous solution that initially contains the racemic feed solution and the aqueous stripping solution. Transportation of (*S*)-amlodipine occurs as a consequence of the concentration driving force between the two opposite sides of aqueous phase.

The (*S*)-amlodipine can be separated after derivatization [35] (diastereoisomeric esters or a diastereoisomeric salt) or, in one step, by complex formation [36]. The good complex-forming abilities of enantiomeric compound and (+)-DBTA arise from a number of facts [37-39]. The carboxylic acid groups of amlodipine and (+)-DBTA can donate protons for hydrogen bonding while they can also behave as a proton acceptor due to the eight oxygen atoms they contain [40-42]. The benzoyl groups can take part in hydrophobic interactions while the other parts of the molecule contain polar hydrophilic groups [43-44].

Although (+)-DBTA is the most frequently used, widely available and cheap acidic resolving agents, it has a low distribution ratio when extracting racemic amlodipine from an aqueous phase to an organic phase [45]. Recently, combination of extractants of D2EHPA and (+)-DBTA can form new complexes, which can be used as chiral selectors for the resolution of enantiomeric compound and both showed good enantioselectivity and a high distribution ratio [46, 47].

In this work, the mixture of synergistic enantioselector achiral extractant D2EHPA and a chiral extractant (+)-DBTA resided in the liquid membrane, trapped in the hydrophobic microporous hollow fiber module. The synergistic enantioselector compound forms enantioselective complexes with (*S*)-amlodipine by hydrogen bonding. Previous partitioning experiments [21] indicate that (*R*)-amlodipine prefers to remain in the feed phase whereas the (*S*)-amlodipine-extractant complex dissolves in the membrane phase. However, the equilibrium constant (K_{ex}) of complex is far bigger than the distribution coefficient, so the influence on mass transfer is small and can generally be neglected. The transport mechanism of (*S*)-amlodipine through the

liquid membrane by using (+)-DBTA as a chiral selective extractant is schematically shown in Figure 4.2(a), while the mechanism of the achiral extractant using D2EHPA is shown in Figure 4.2(b). Consequently, the novel synergistic enantioseparation of (*S*)-amlodipine by using chiral selective extractant, *O*,*O*'-dibenzoyl-(2*S*,3*S*)-tartaric acid ((+)-DBTA) and an achiral extractant, di(2-ethylhexyl)phosphoric acid (D2EHPA) is illustrated in Figure 4.2(c).

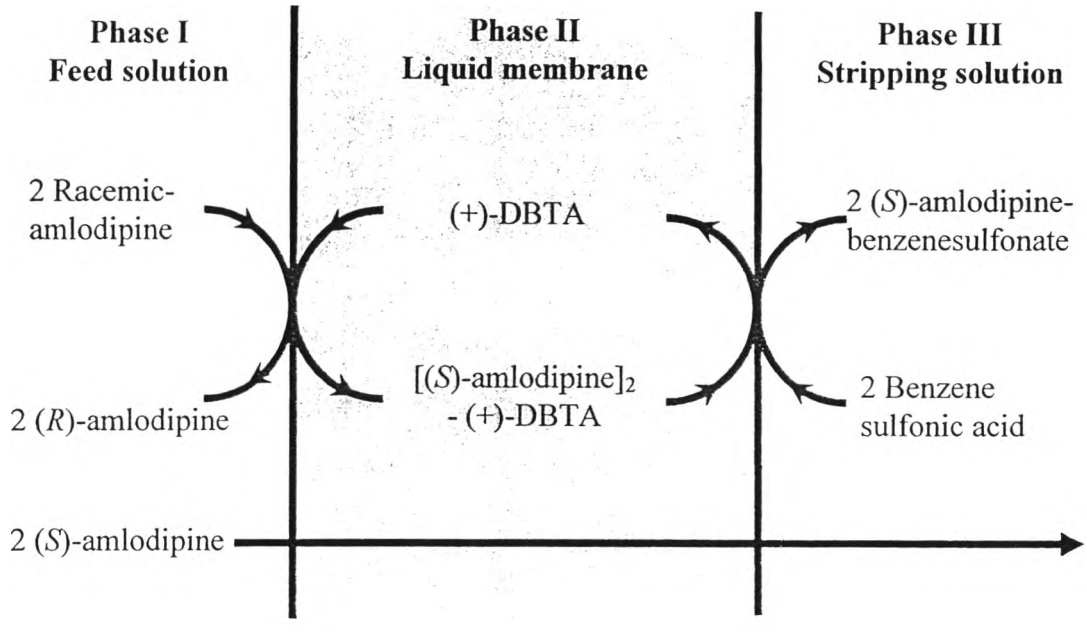

(a)

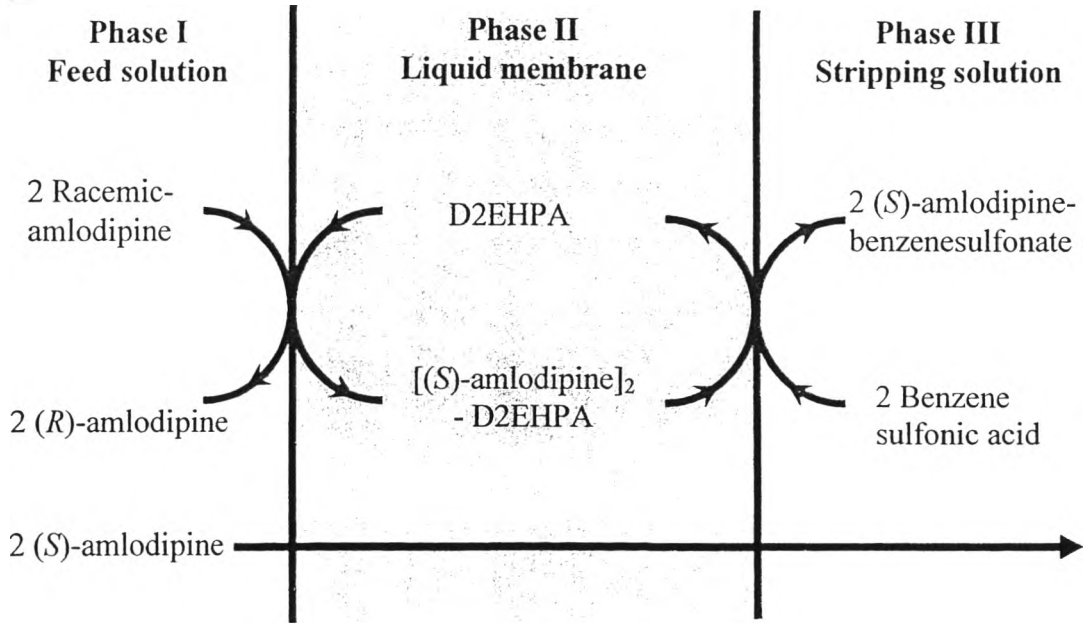

(b)

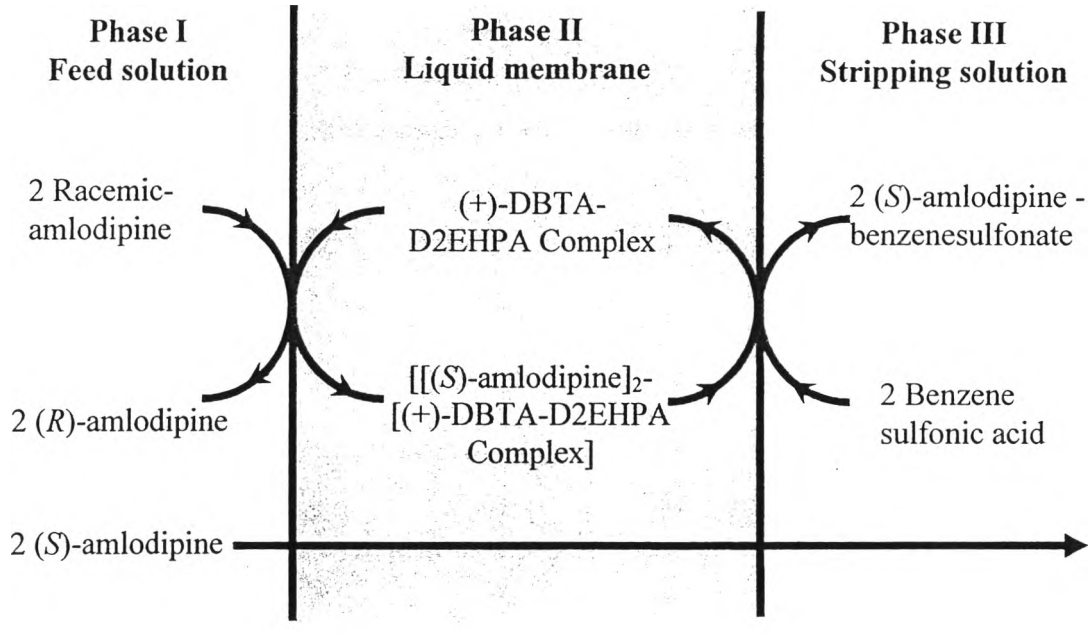

(c)

Figure 4.2 (a) The counter transport mechanism of (*S*)-amlodipine using (+)-DBTA as the chiral selective extractant

(b) The counter transport mechanism of (*S*)-amlodipine using D2EHPA as extractant

(c) The counter transport mechanism of (*S*)-amlodipine using (+)-DBTA-D2EHPA Complex as the synergistic extractant

The extraction reaction of (*S*)-amlodipine with an only chiral discrimination ((+)-DBTA), forming (*S*)-amlodipine-(+)-DBTA complex is shown in Eq. (4.1).

$$2[(S)\text{-amlodipine}]_f + [(+)\text{-DBTA}]_m \underset{k_2}{\overset{k_1}{\rightleftharpoons}} [[(S)\text{-amlodipine}]_2\text{-}(+)\text{-DBTA}]_m \quad (4.1)$$

where k_1 and k_2 are the apparent reaction rate constants of the feed membrane interfacial and membrane strip interfacial transport of (*S*)-amlodipine, respectively. Define the suffixes, f and m, as feed phase and membrane phase, respectively.

The extraction of (*S*)-amlodipine with an achiral carrier (D2EHPA) was reacted by the cation-exchange reaction and proton-transfer reaction as shown in Eq. (4.2).

$$2[(S)\text{-amlodipine}]_f + [\text{D2EHPA}]_m \underset{k_4}{\overset{k_3}{\rightleftharpoons}} [[(S)\text{-amlodipine}]_2\text{- D2EHPA}]_m \quad (4.2)$$

where k_3 and k_4 are the apparent reaction rate constants of the feed membrane interfacial and the membrane strip interfacial transport of (*S*)-amlodipine, respectively. Define the suffixes, f and m, as feed phase and membrane phase, respectively.

4.3.2 Synergistic extraction theory

Synergistic separation is the phenomenon in which two extractants taken together extracted a target compound. Synergistic separation is an important method to enhance the extraction efficiency [48] and has been applied for extraction and separation of many compounds [49]. It has much higher efficiency as compared to the normal additive effect of these extractants separately [50]. By using a mixture of the selected extractants with favor on specific forms, synergistic extraction is the great interest used on the separation of enantiomer such as (*S*)-amlodipine. The extraction reaction of (+)-DBTA mixed with D2EHPA is shown in Figure 4.2(c). Figure 4.2(c) shows the descriptive schematic mechanisms of (*S*)-amlodipine with the synergistic extractant and stripping solution. The complex species react with the stripping solution.

The synergistic extraction of (*S*)-amlodipine by a mixture of the chiral agent (+)-DBTA and the achiral carrier (D2EHPA) occurred because there are two extraction reactions in the system. The primary reaction is the reaction between a chiral discrimination ((+)-DBTA) and achiral carrier (D2EHPA) which forms the extractant complex ((+)-DBTA-D2EHPA) as shown in Eq. (4.3) [51]. The secondary reaction is the reaction between the extractant complex ((+)-DBTA-D2EHPA) and (*S*)-amlodipine. This reaction takes place at the presence of proton transfer-chiral interactions, i.e. (+)-DBTA-D2EHPA as shown in Eq. (4.3) and Eq. (4.4). It produces the derivative complex, namely (*S*)-amlodipine-(+)-DBTA-D2EHPA.

$$[(+)\text{-DBTA}]_m + [\text{D2EHPA}]_m \underset{k_6}{\overset{k_5}{\rightleftharpoons}} [(+)\text{-DBTA-D2EHPA}]_m \quad (4.3)$$

$$2[(S)\text{-amlodipine}]_f + [(+)\text{-DBTA-D2EHPA}]_m \quad (4.4)$$

$$\underset{k_8}{\overset{k_7}{\rightleftharpoons}} [[(S)\text{-amlodipine}]_2\text{-}[(+)\text{-DBTA-D2EHPA}]]_m$$

where k_5 and k_6 are the apparent reaction rate constants of formed extractant and unformed extractant, respectively. k_7 and k_8 are the apparent reaction rate constants of the feed membrane interfacial and the membrane strip interfacial transport of (*S*)-amlodipine, respectively. Define the subscript, f and m, mean feed phase and membrane phase, respectively.

In the presence of benzenesulfonic acid in the stripping phase, benzenesulfonic acid reacts with $[[(S)\text{-amlodipine}]_2\text{-}(+)\text{-DBTA}]_m$ to recover (*S*)-amlodipine into the stripping phase:

$$[[(S)\text{-amlodipine}]_2\text{-}[(+)\text{-DBTA-D2EHPA}]]_m + 2[\text{benzenesulfonic acid}]_s \quad (4.5)$$

$$\underset{k_{10}}{\overset{k_9}{\rightleftharpoons}} 2[(S)\text{-amlodipine-benzenesulfonate}]_s + [\text{-}(+)\text{-DBTA-D2EHPA}]_m$$

where k_9 and k_{10} are the apparent reaction rate constants of the membrane-strip interfacial and strip-membrane interfacial transport of amlodipine enantiomer, respectively. Define the suffixes, m and s, as membrane phase and stripping phase, respectively.

The aspect of synergistic effects is captured. The highest extraction of (*S*)-amlodipine occurs at extractant concentrations of 4 mmol/L (+)-DBTA and 4 mmol/L D2EHPA. The effect of synergistic extraction (expressed as synergistic coefficient, S.C.) as a function of the distribution ratio is shown [52]:

$$S.C = \frac{D.R._{12}}{(D.R._1 + D.R._2)} \quad (4.6)$$

where $D.R._{12}$ is a distribution ratio from the synergistic extractant. $D.R._1$ or $D.R._2$ are distribution ratios obtained from a single extraction.

It is calculated that S.C for (*S*)-amlodipine was 1.50 under 4 mmol/L (+)-DBTA mixed with 4 mmol/L D2EHPA.

4.3.3 Extraction equilibrium constant and the distribution ratio

The extraction equilibrium constant (K_{ex}) of (*S*)-amlodipine extracted by [(+)-DBTA in Eq. (4.7) was derived from the experimental data and calculated as follow.

From the extraction reaction described in Eq. (4.3) and (4.4), the extraction equilibrium constant (K_{ex}) can be expressed as

$$K_{ex} = \frac{[[(S)\text{-amlodipine}]_2\text{-}(+)\text{-DBTA-D2EHPA}]_{m,f}}{[(S)\text{-amlodipine}]^2_{f,m}[(+)\text{-DBTA}]_{m,f}[\text{D2EHPA}]_{m,f}} \quad (4.7)$$

The distribution ratio (*D*) for (*S*)-amlodipine by definition of distribution ratio from IUPAC compendium of chemical terminology [53], was given by

$$D = \frac{[[(S)\text{-amlodipine}]_2\text{-}(+)\text{-DBTA-D2EHPA}]_{m,f}}{[(S)\text{-amlodipine}]_{f,m}} \quad (4.8)$$

According to Eq. (4.8), the distribution ratio could then be derived as a function of the extraction equilibrium constant as follows:

$$D = K_{ex}[(S)\text{-amlodipine}]_{f,m}[(+)\text{-DBTA}]_{m,f}[\text{D2EHPA}]_{m,f} \quad (4.9)$$

From the stripping reaction described in Eq. (4.5), the stripping equilibrium constant (K_{st}) can be expressed as

$$K_{st} = \frac{[(S)\text{-amlodipine-benzenesulfonate}]^2_{s,m}[(+)\text{-DBTA-D2EHPA}]_{m,s}}{[[(S)\text{-amlodipine}]_2\text{-}(+)\text{-DBTA-D2EHPA}]_{m,s}[\text{benzenesulfonate}]^2_{s,m}} \quad (4.10)$$

where the value of K_{ex} for (*S*)-amlodipine extracted with (+)-DBTA-D2EHPA complex and K_{st} for (*S*)-amlodipine stripped with benzenesulfonic acid were found to be 0.7642 $L^3/mmol^3$ and 1.4839, respectively. The results of experiment were showed in section 4.5.11.

In this work, the extractability of (*S*)-amlodipine was determined by the percentage of extraction:

$$\%\text{Extraction} = \frac{C_{f,in} - C_{f,out}}{C_{f,in}} \times 100 \tag{4.11}$$

The percentage of recovery was calculated by

$$\%\text{Stripping} = \frac{C_{s,out}}{C_{f,in}} \times 100 \tag{4.12}$$

where $C_{f,in}$ and $C_{f,out}$ are the concentrations of component *i* (mmol/L) in the inlet feed and outlet, respectively, and $C_{s,out}$ is the concentrations of component *i* (mmol/L) in the outlet stripping.

The selectivity is defined as enantioselectivity. The enantioselectivity of the membrane process is given in terms of enantiomeric excess. The enantiomeric excess is defined by the ratio of the difference between the concentrations of both enantiomers in the feed or stripping phase to the total amount of both enantiomers present at any time, and was calculated according to Eq. (4.13):

$$\%\text{Enantiomeric excess} = \frac{C_{(S)} - C_{(R)}}{C_{(S)} + C_{(R)}} \times 100 \tag{4.13}$$

4.3.4 Permeability coefficient

The permeation of (*S*)-amlodipine can be expressed in terms of the permeability coefficient (*P*) as proposed by Danesi [54] in Eq. (4.14):

$$-V_f \ln\left(\frac{C_f}{C_{f,o}}\right) = AP\frac{\beta}{\beta+1}t \tag{4.14}$$

$$\beta = \frac{Q_f}{PL\varepsilon\pi N r_i} \tag{4.15}$$

where P is the permeability coefficient (cm/s), V_f is the volume of the feed (cm^3), $C_{f,0}$ is the (*S*)-amlodipine concentration (mmol/L) in initial time (t = 0), C_f is the (*S*)-amlodipine concentration at time t (mmol/L), A is the effective area of the hollow fiber module (cm^2), t is the time (min), Q_f is the volumetric flow rate of feed solution (cm^3/s), L is the length of the hollow fiber (cm), ε is the porosity of the hollow fiber (%), N is the numbers of hollow fibers in the module and r_i is the internal radius of the hollow fiber (cm).

$AP(\beta/(\beta+1))$ is the slope of the plot between $-V_f \ln (C_f/C_{f,0})$ versus time (t) in Eq. (4.14), and P can be obtained by Eq. (4.15). To determine mass transfer coefficients for (*S*)-amlodipine enantioseparation by HFSLM, the mass-transfer model and permeability coefficient (P) are employed. The permeability coefficient depends on mass-transfer resistance which is the reciprocal of the mass-transfer coefficients as follows:

$$\frac{1}{P} = \frac{1}{k_f} + \frac{r_i}{r_{lm}}\frac{1}{P_m} + \frac{r_i}{r_o}\frac{1}{k_s} \tag{4.16}$$

where r_{lm} is the log-mean radius of the hollow fiber, r_o is the external radius of the hollow fiber (cm), k_f is the aqueous mass-transfer coefficient in tube side, k_s is the stripping mass-transfer coefficient in shell side and P_m is the membrane permeability coefficient.

The relation between P_m and the distribution ratio (D) are as follows:

$$P_m = Dk_m \tag{4.17}$$

Combining Eq. (4.9) and Eq. (4.17), thus

$$P_m = K_{ex}\, k_m [(S)\text{-amlodipine}]_f [(+)\text{-DBTA}]_m [\text{D2EHPA}]_m \tag{4.18}$$

where k_m is the mass-transfer coefficient of membrane, a value of liquid-membrane permeability coefficient (P_m) from Eq. (4.18) is substituted into Eq. (4.16). Assuming that the stripping reaction is instantaneous and the contribution of the stripping phase is neglected. Eq. (4.16) becomes:

$$\frac{1}{P} = \frac{1}{k_f} + \frac{r_i}{r_{lm}} \frac{1}{K_{ex}\, k_m [(S)\text{-amlodipine}]_f [(+)\text{-DBTA}]_n [\text{D2EHPA}]_n} \tag{4.19}$$

where k_f is the mass-transfer coefficient of the feed solution.

4.4 EXPERIMENT

4.4.1 Chemicals and reagents

The aqueous phase was pharmaceutical wastewater containing racemic amlodipine (Government Pharmaceutical Organization (GPO), Bangkok, Thailand). (*R*)-amlodipine, (*S*)-amlodipine and racemic amlodipine, all of pharmaceutical grade, were provided from the Government Pharmaceutical Organization (GPO) of Thailand. The organic phase was a solution of the synergistic extractant ((+)-DBTA+D2EHPA) in 1-octanol an analytical reagent grade obtained from Merck, Germany. (+)-DBTA was obtained from Acros, USA as chiral selectors, D2EHPA (Acros Organics, USA) as a cationic carrier. The stripping solution benzenesulfonic acid (Sigma-Aldrich, St. Louis, USA) was dissolved in deionized water (Millipore®, USA). The solvents, i.e. *N,N*-dimethylformamide, cyclohexane, 1-decanol and 1-propanol, were all of analytical reagent grade and were obtained from Merck, Germany. All reagents used

in this experiment were of GR grade and also were purchased from Merck, Germany. Aqueous solutions were prepared using Milli-Q® deionized water (Millipore®, USA). Doubly deionized water was used throughout the experiments.

4.4.2 Apparatus

The hollow fiber supported liquid membrane (HFSLM) system (Liqui-Cel® Extra-flow 2.5 in. × 8 in. membrane contactor) was manufactured by Hoechst Celanese, USA. The module uses Celgard® microporous polypropylene fibers that are woven into fabric and wrapped around a central tube feeder that supplies the shell-side fluid. The woven fabrics provided more uniform fiber spacing, which in turn leads to higher mass-transfer coefficients than those obtained with individual fibers [55]. The properties of the hollow-fiber module are specified in Table 4.1. The fibers were put into a solvent-resistant polyethylene tube sheet and shell casing in polypropylene.

4.4.3 Procedures

The single-module operation is shown in Figure 4.3. The selected organic carrier (+)-DBTA, D2EHPA and synergistic extractant ((+)-DBTA+D2EHPA) were dissolved in 1-decanol (500 mL) individually. The extractant was simultaneously pumped into the tube and shell sides of the hollow-fiber module for 40 min to ensure the extractant was entirely embedded in micropores of the hollow fibers. Subsequently, 5 L of feed solution and stripping solution were fed counter-currently into the tube side and the shell side of the single-module operation, respectively.

The concentration of selected organic carrier (+)-DBTA, D2EHPA and synergistic extractant ((+)-DBTA+D2EHPA) in the liquid membrane was deliberately varied to find the optimum value for (*S*)-amlodipine separation. The volumetric flow rates of feed and stripping solutions, the number of separation cycles, and stability of HFSLM were each investigated in turn. The operating time for each run was 50 min. The concentrations of (*S*)-amlodipine in samples from the feed and stripping solutions were determined by high-performance liquid chromatography (HPLC) in accordance with United States Patent No US 6646131 B2 [56] to estimate the percentages of

extraction and stripping. To achieve higher enantioseparation and to study membrane stability, the number of separation cycles was varied. The feed of the second cycle was obtained from the first outlet feed solution and so on, whereas the inlet stripping solution was fresh.

Table 4.1 The properties of the hollow-fiber module

Properties	Descriptions
Material	Polypropylene
Inside diameter of hollow fiber	240 μm
Outside diameter of hollow fiber	300 μm
Effective length of hollow fiber	15 cm
Number of hollow fibers	35,000
Average pore size	0.03 μm
Porosity	30%
Effective surface area	1.4×10^4 cm^2
Area per unit volume	29.3 cm^2/cm^3
Module diameter	6.3 cm
Module length	20.3 cm
Contact area	30%
Tortuosity factor	2.6
Operating temperature	273.15-333.15 K

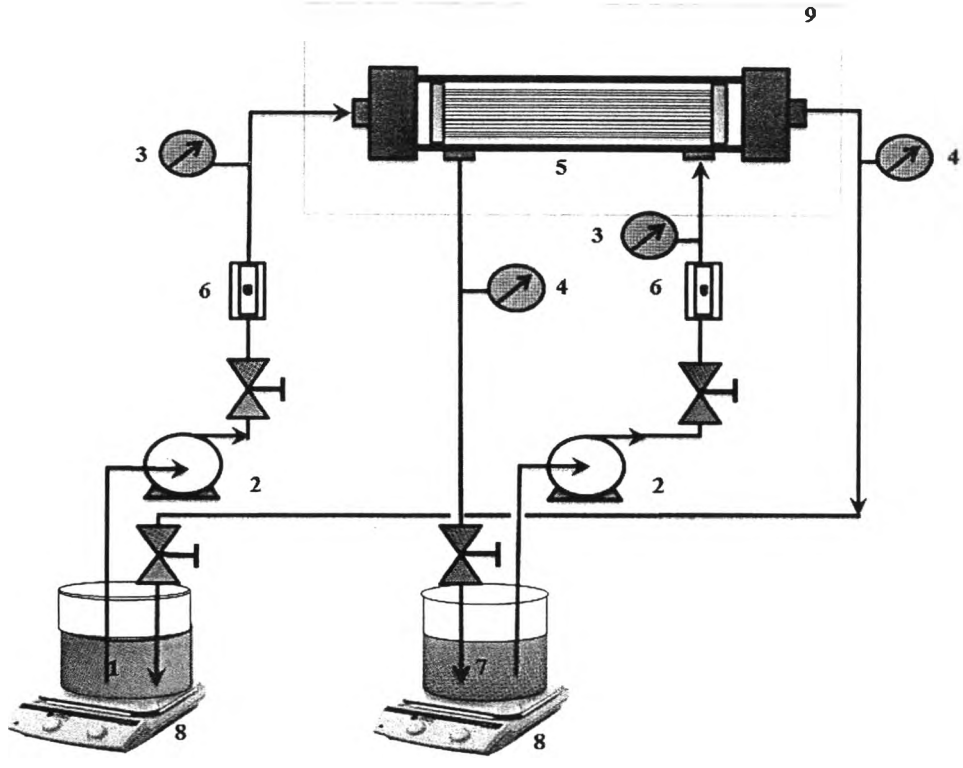

Figure 4.3 Schematic representation of the counter-current flow diagram for batch-mode operation in HFSLM: 1) feed reservoir, 2) gear pumps, 3) inlet pressure gauges, 4) outlet pressure gauges, 5) the hollow-fiber module, 6) flow meters, 7) stripping reservoir, 8) stirrer with temperature controller, and 9) temperature control box

4.4.4 Analytical instruments and chromatographic conditions

Chiral chromatography was performed on Agilent® 1100 Compact LC system series (Agilent Technologies, Palo Alto, CA, USA). The chromatographic system was equipped with Agilent® 1100 Compact LC system series (Agilent Technologies, Palo Alto, CA, USA). The chromatographic system used was equipped with an in-built solvent degasser, a quaternary pump, a column compartment, a photodiode array detector with variable injector and an auto sampler. Data analysis was carried out using Chemstation® Version B.04.01 software.

The chromatographic procedure was carried out by using chiral column ultron ES-OVM, Ovomucoid column (5 μm, 4.6 × 150 mm) [56]. The column temperature was controlled at 298.15 K by using a column heater. The mobile phase

was prepared by mixing of disodium hydrogen phosphate buffer (20 mmol/L) and acetonitrile (80:20 %v/v). The flow rate of the mobile phase was 0.3 ml/min. Injection volume was 20 μL. The sample was detected with UV 237 nm while the relative retention time of (*R*)-amlodipine was about 1.0 and (*S*)-amlodipine was about 1.2. The analysis time was set at 20 min per sample to eliminate potential interference from late eluting peaks. The pH of the aqueous phase was measured with a pH meter model: SevenMulti™ Modular Expansion (Mettler-Toledo, Greifensee, Switzerland).

4.5 RESULTS AND DISCUSSION

According to the suggested mechanism in the synergistic extraction of enantiomeric compound, the pH value in the aqueous phase, the extractant composition, the concentration of stripping solution, the flow rates of feed and stripping solution, the number of separation cycles and the temperature could influence the separation efficiency. To make the experiment data comparable, the pH in aqueous phase was fixed. The influences of the other factors were studied.

4.5.1 The effect of the pH of the feed phase

By varying the pH of the feed solution in Figure 4.4, the results were clearly seen that the percentage of (*S*)-amlodipine extraction, the enantiomeric excess (% *e.e.*) increased with increasing of pH until 5.0. Then, it gradually decreases. This influence of pH of the feed solution was similar to our previous work [21]. The reasons can be explained by the fact that the ratio between protonated and unprotonated amlodipine decreases with the rise of pH value. Ionic amlodipine only exists in aqueous phase. At pH 5.0, the enantiomers of amlodipine are expected to be unprotonated because the pKa of amlodipine is about 8.6 at 298.15 K [21, 57]. When pH values are higher than 5.0, amlodipine exists in the form of neutral molecule, (*S*)-amlodipine and (*R*)-amlodipine were increased and able to enter the membrane phase. The enantiomeric excess (% *e.e.*) decreased because the membrane phase did not perfectly extract only (*S*)-amlodipine into the membrane phase and eliminated (*R*)-amlodipine into the feed solution. So, pH 5.0 was an appropriate choice in view of the bigger enantioselectivity of the enantioselective extraction. The highest selective extraction of (*S*)-amlodipine

by the synergistic extractant in a single-module operation of 80.04% was obtained at the pH of 5.0.

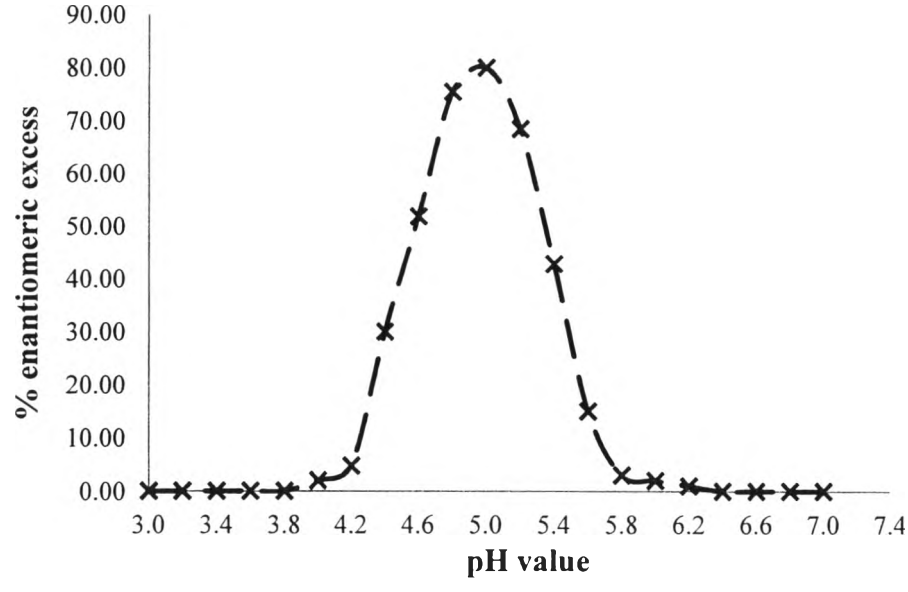

Figure 4.4 The effect of pH on the percentages of enantiomeric excess (% *e.e.*)

4.5.2 The effect of chiral selector concentration in liquid membrane

The transport of (*S*)-amlodipine from the feed solution through liquid membrane that contains (+)-DBTA as the chiral selective extractant is a counter-transport process [58]. The dependence of the percentage of extraction of (*S*)-amlodipine with (+)-DBTA concentration is shown in Figure 4.5(a). The highest percentage of (*S*)-amlodipine extraction about 84.50% was obtained at the concentration around 4 mmol/L and it was recorded as the optimized concentration to use in a further run. However, in this work, when (+)-DBTA concentration is higher than 4 mmol/L, the percentage of extraction decreases due to an excessive increase in extractant concentration which produces an increase in the absolute viscosity of the membrane [59]. According to the molecular kinetic interpretation of Nernst, the diffusion coefficient (D_c) can be defined as [60]:

$$D_c = \frac{k_B T}{6\pi\eta r} \tag{4.20}$$

where k_B is Boltzman's constant, η is the viscosity of the liquid membrane, r and T are the radius and temperature, respectively. All of these results also occur in the stripping phase as shown in Figure 4.5(a). High selectivity of (*S*)-amlodipine was obtained.

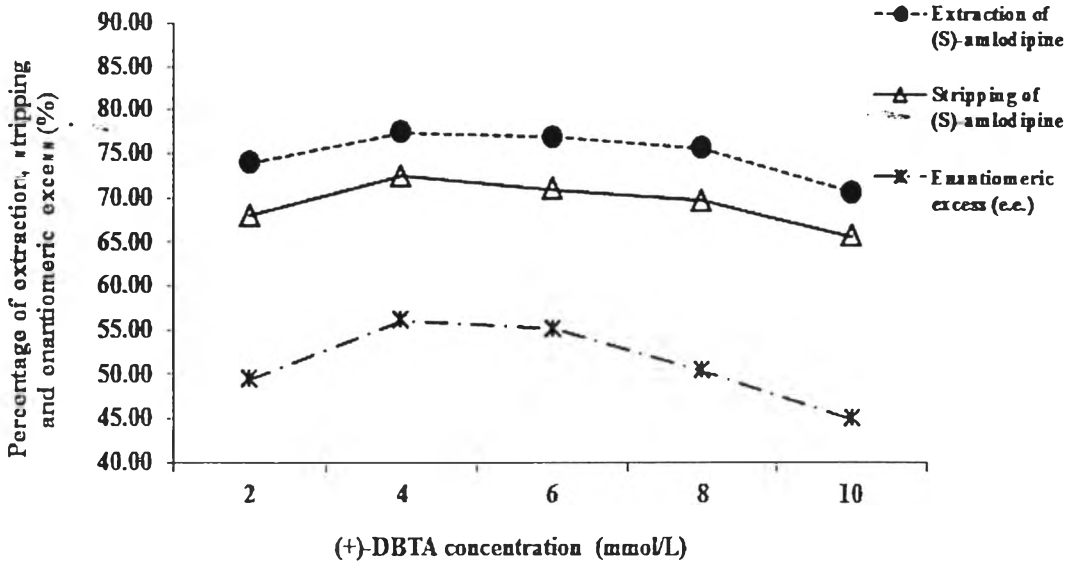

(a)

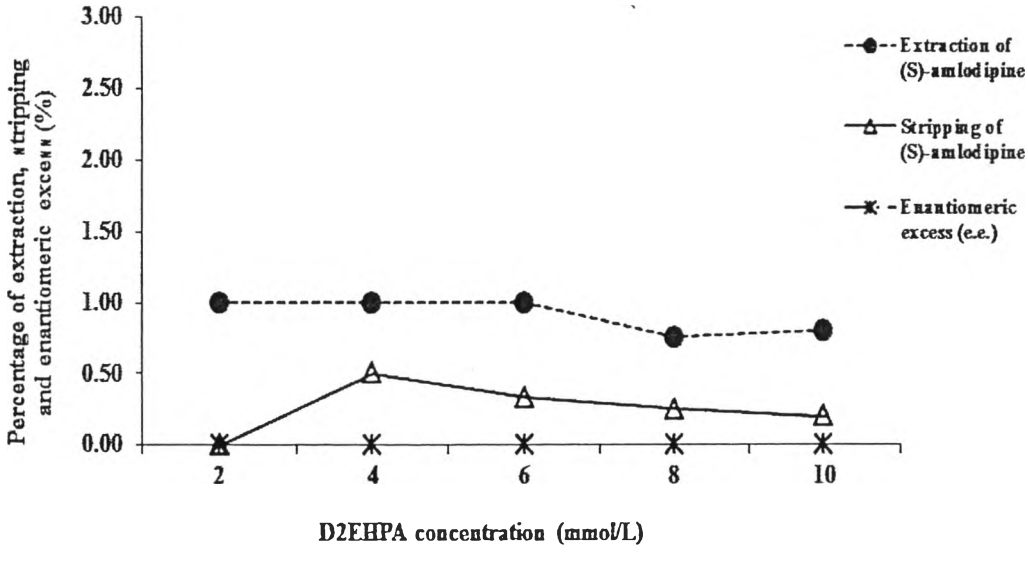

(b)

Figure 4.5 (a) The effect of the chiral selective extractant ((+)-DBTA) on percentages of extraction and recovery of (*S*)-amlodipine and % *e.e.*

(b) The effect of D2EHPA on percentages of extraction and recovery of (*S*)-amlodipine and % *e.e.*

4.5.3 The effect of achiral extractant concentration in liquid membrane

The achiral carrier (D2EHPA) is a cationic extractant. The mechanisms of D2EHPA to extract (*S*)-amlodipine by using the cation-exchange reaction and proton-transfer reaction are shown in Figure 4.5(b). Figure 4.2(b) represents the extraction reaction of (*S*)-amlodipine via D2EHPA extractant.

From Figure 4.5(b), D2EHPA concentrations of 2–10 mmol/L slightly extracted and stripped (*S*)-amlodipine. D2EHPA results in poor extraction of (*S*)-amlodipine and the mass-transfer rate. However, in this case, the percentage of the extraction was low because D2EHPA is an achiral extractant. Without the chiral selective group, the eantiomeric substances could not react with D2EHPA. Thus, the extraction and stripping in the presence of achiral extractant by D2EHPA alone was poor.

4.5.4 The synergistic effects of the combination of chiral selective extractant and achiral extractant

The influences of the synergistic extractant compositions were summarized in Figure 4.6. When D2EHPA was not added to the extractant, (+)-DBTA showed enantioselectivity on racemic amlodipine, but with very small value. With the increase of the D2EHPA content, the percentage of enantiomeric excess of (*S*)-amlodipine was greatly enhanced. Meanwhile, the enantioselectivities all increased before the concentration of D2EHPA was up to 4 mmol/L. The concentration of D2EHPA further increased, the percentage of enantiomeric excess continuously increased, while the enantioselectivities followed an opposite tendency. This is because D2EHPA does not have chiral separation ability, but it has a high extraction capacity. So when there is more D2EHPA, the selectivity will be less. Figure 4.5 (a) shows the influence of the concentration of (+)-DBTA on the separation efficiency. When no chiral selector was added to the extractant, the percentage of enantiomeric excess of (*S*)-amlodipine was 70.21%, although no enantioselectivity was found. With an increase of the concentration of (+)-DBTA, the percentage of enantiomeric excess of (*S*)-amlodipine was kept to a moderate extent and showed no obvious trend.

However, the enantioselectivities increased steadily. The optimized condition is the concentration ratio between (+)-DBTA: D2EHPA of 1:1.

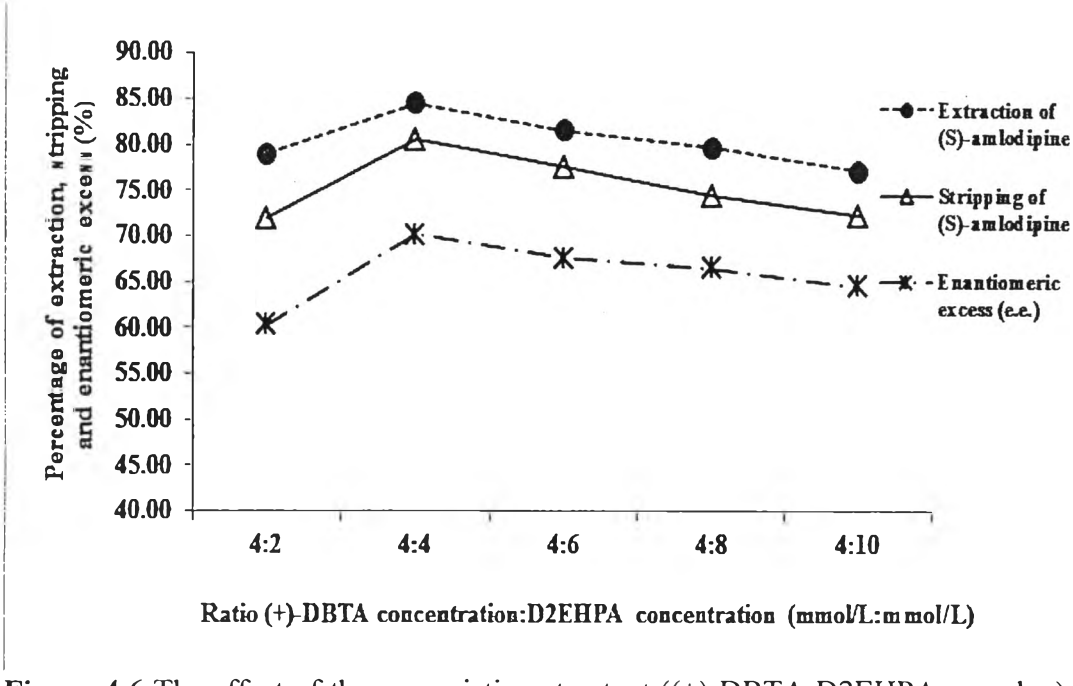

Figure 4.6 The effect of the synergistic extractant ((+)-DBTA-D2EHPA complex) on percentages of extraction and recovery of (*S*)-amlodipine and % *e.e.*

4.5.5 The effect of stripping-phase concentration

The effects of benzenesulfonic acid concentration in the stripping solution on the efficiency of (*S*)-amlodipine recovery were also investigated and results were shown in Figure 4.7. The concentrations of benzenesulfonic acid, a stripping solution, were studied at 2, 4, 6, 8 and 10 mmol/L on the percentage of extraction, stripping and enantiomeric excess in the stripping process of (*S*)-amlodipine. The chiral selector used 4 mmol/L (+)-DBTA and 4 mmol/L D2EHPA. Figure 4.4 is evident for very strong influence of pH of the feed phase on the percentage of enantiomeric excess. The maximum % *e.e.* at the pH of 5.0 is explained by the formation of unprotonated enantiomers of amlodipine. However, the pH of stripping phase can be influenced by the concentration of benzenesulfonic acid in the stripping solution. From Figure 4.7, benzenesulfonic acid accelerates the stripping process, but similarly as in Figure 4.4, at higher concentrations in the stripping solution, stripping process of (*S*)-amlodipine decreases. This reason is the same as that in section 4.5.1. From Figure 4.7, for single-

module operation, the highest stripping of (*S*)-amlodipine about 80.50% was achieved at the benzenesulfonic acid concentration of 4 mmol/L. This concentration (4 mmol/L) will be referred for the next study run in an attempt to establish the highest possible (*S*)-amlodipine recovery.

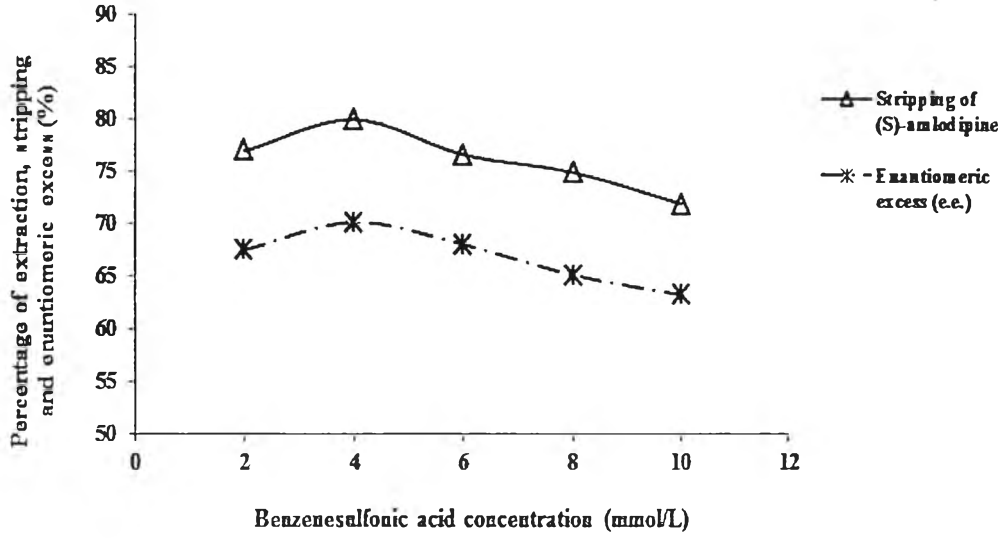

Figure 4.7 The effect of stripping solution concentration on percentages of recovery of (*S*)-amlodipine and % *e.e.*

4.5.6 The effect of the flow rate of feed solution

The flow rate during extraction is an important factor. The effects of flow rate on the extraction of (*S*)-amlodipine were shown in Figure 4.8. Figure 4.8 showed the relationship between the percentage of extraction and stripping of (*S*)-amlodipine, and the enantiomeric excess at the equal flow rates of feed and stripping solutions at 50, 100, 150 and 200 mL/min with the counter-flow pattern were studied. The extractant used was 4 mmol/L of (+)-DBTA and 4 mmol/L of D2EHPA and the concentration of stripping solution was 4 mmol/L. The results indicate that by using the flow rates of feed solutions of 100 ml/min, the highest percentage of the extraction of (*S*)-amlodipine about 84.50% was obtained. The flow rates of feed solutions tremendously play an important role on the percentages of extraction and stripping of (*S*)-amlodipine. Too high flow rates result in less resident time of the solutions or less contact time of the relevant molecules in the reaction in the HFSLM process. In other

words, too high flow rates, especially at 200 mL/min, may cause the deterioration of the membrane system which can be seen from poor liquid-membrane stability and lower percentage of extraction [61, 62].

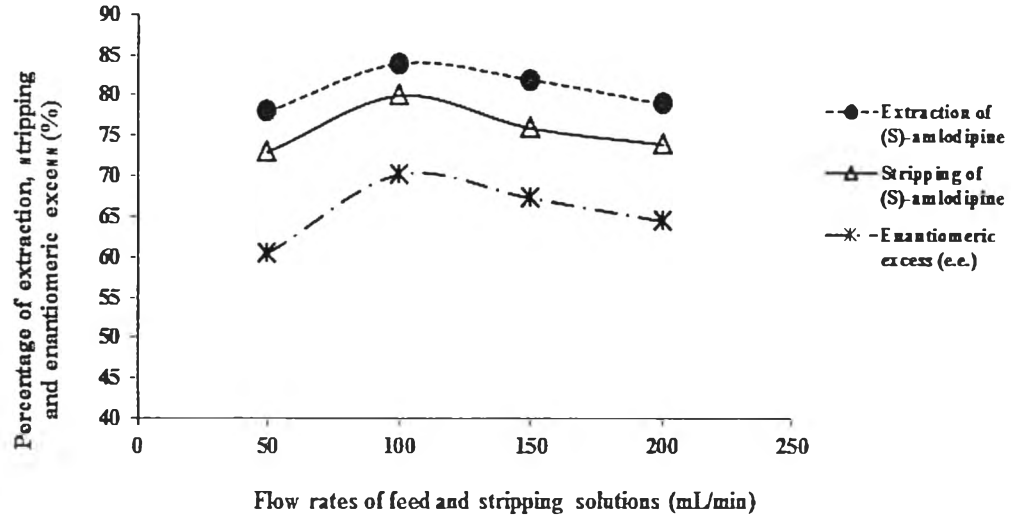

Figure 4.8 The effects of the flow rates of feed and stripping solution on percentages of extraction and recovery of (*S*)-amlodipine and % *e.e.*

4.5.7 The effect of the flow rates of stripping solution

The effects of flow rate of the stripping solution through the hollow-fiber module were investigated. It is an important parameter that influences the performance of (*S*)-amlodipine recovery. Figure 4.8 shows the plot of percentages of (*S*)-amlodipine stripping versus flow rates of stripping solution. The flow rates of the stripping solution were varied between 50 - 200 mL/min with the operating time of 50 min. The results indicated that at the flow rate of stripping solution of 100 mL/min, the highest percentages of (*S*)-amlodipine stripping of 80.50% was obtained. However, the percentage of (*S*)-amlodipine extraction and stripping decreased with an increase of the flow rates of the feed and stripping solutions due to the resident time of solution in the hollow-fiber module.

4.5.8 The effect of number of separation cycle through the hollow-fiber module

The numbers of separation cycles were studied using the optimum conditions in a single-module operation to expect the possible highest separation. Besides, this study indicated the least possible (*S*)-amlodipine concentration in the feed as well as the membrane stability. Figure 4.9 shows that the percentages of (*S*)-amlodipine cumulative extraction and cumulative stripping were obtained at 6-cycle operation for 300 min. The cumulative extraction and stripping reached 84.90% and 80.80%, respectively.

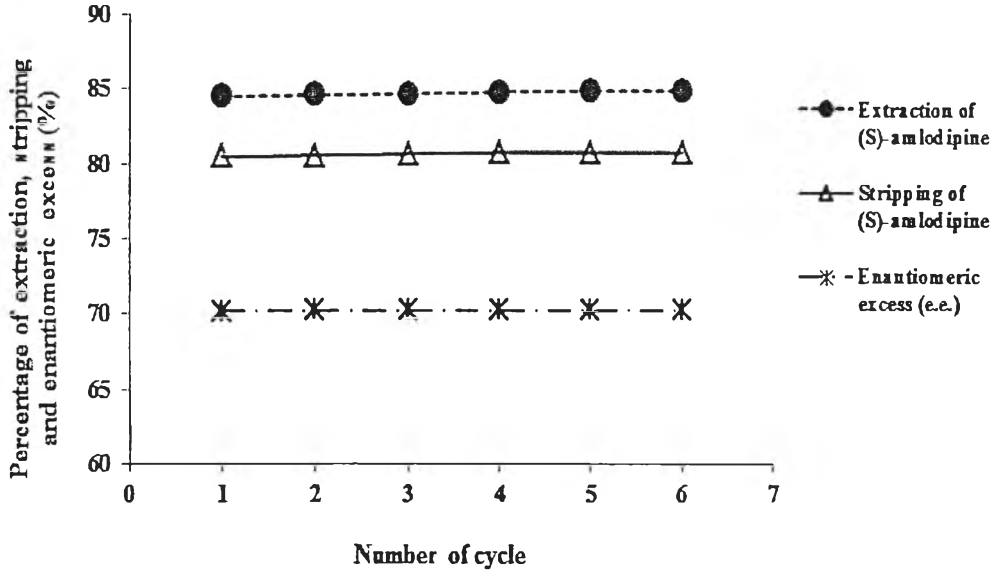

Figure 4.9 The effect of number of separation cycle through the hollow-fiber module on percentages of extraction and recovery of (*S*)-amlodipine and % *e.e.*

4.5.9 The effect of temperature on percentages of extraction, stripping and enantiomeric excess

The effects of temperature on stripping solution were studied at 278.15, 283.15, 288.15, 293.15, 298.15, 303.15, 308.15 and 313.15 K to investigate the effect of temperature on the percentages of extraction, stripping and enantiomeric excess as

shown in Figure 4.10. The optimum conditions were the pH of 5.0 in feed solution, 4 mmol/L of (+)-DBTA and 4 mmol/L of D2EHPA, 4 mmol/L benzenesulfonic acid, the feed flow rate of 100 ml/min and the stripping flow rate of 100 ml/min. From Figure 4.10, it is observed that enantiomeric excess of (*S*)-amlodipine was increased by decreasing the temperatures. It is found that the highest percentage of enantiomeric excess of (*S*)-amlodipine was 70.21% at the temperature of 278.15 K. The highest percentages of (*S*)-amlodipine extraction and stripping were 84.50% and 80.50%, respectively.

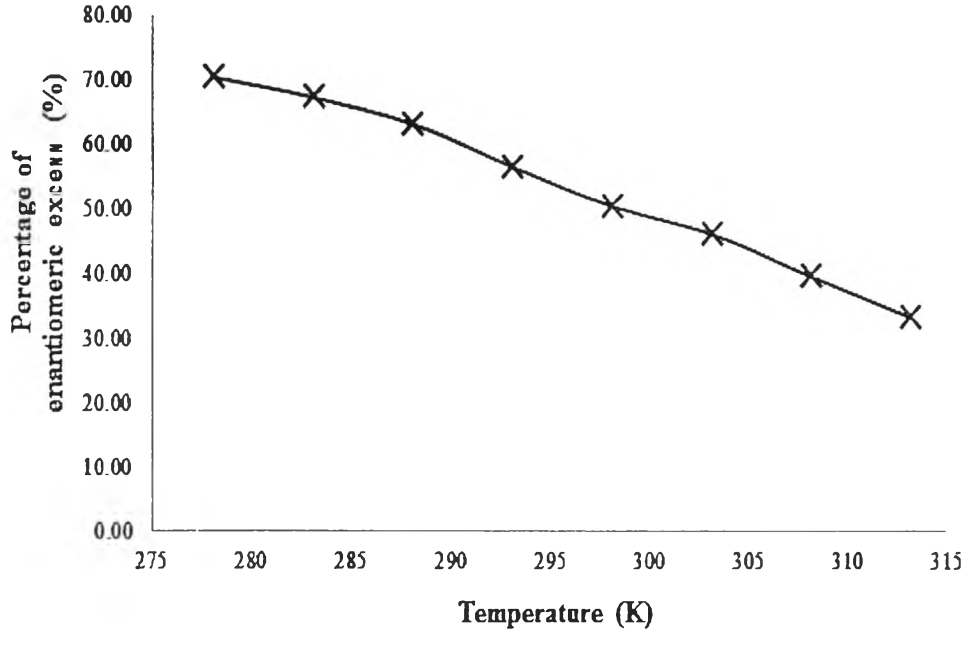

Figure 4.10 The effect of temperature on percentages of % *e.e.*

4.5.10 Van't Hoff's plots of enantioselectivities (α)

The effect of temperature on the enantioselectivities (α) of racemic amlodipine were investigated in the range between 278.15 K and 313.15 K. Table 4.2 shows that a higher temperature leads to a decrease in enantioselectivities (α).

The variations of lnα versus $1/T$ are shown in Figure 4.11. The results can be described as matching very well to the Van't Hoff's model, indicating that the complexes do not change in conformation [63] and that enantioselective interactions also do not change in the temperature range studied [64].

Table 4.2 The effect of temperature on the enantioselectivities (α) of racemic amlodipine

Temperature (K)	α	% e.e.
278.15	5.71	70.21
283.15	5.08	67.10
288.15	4.40	62.98
293.15	3.58	56.29
298.15	3.02	50.30
303.15	2.70	46.01
308.15	2.31	39.58
313.15	2.00	33.30

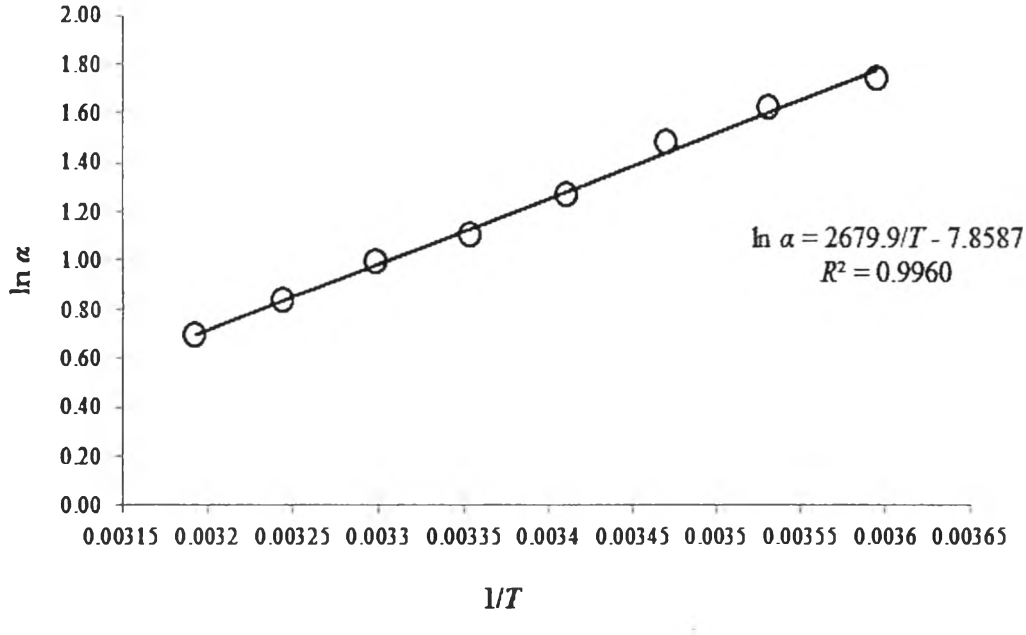

Figure 4.11 The Van't Hoff's plots of enantioselectivities (α)

4.5.11 Extraction equilibrium constant, the stripping equilibrium constant and the distribution ratio

The extraction equilibrium constant (K_{ex}) was calculated by the slope of graph in Figure 4.12(a) and found to be 0.7642 $(L/mmol)^3$. The stripping equilibrium constant (K_{st}) was calculated by the slope of graph in Figure 4.12(b) and found to be 1.4839. The distribution ratio (D) at the (+)-DBTA concentration of 4 mmol/L were calculated by Eq. (4.7) and Eq. (4.10) as shown in Table 4.3. It is noted that the distribution ratio increased with the extractant concentration and agreed with the earlier report by Wannachod *et al.* [65].

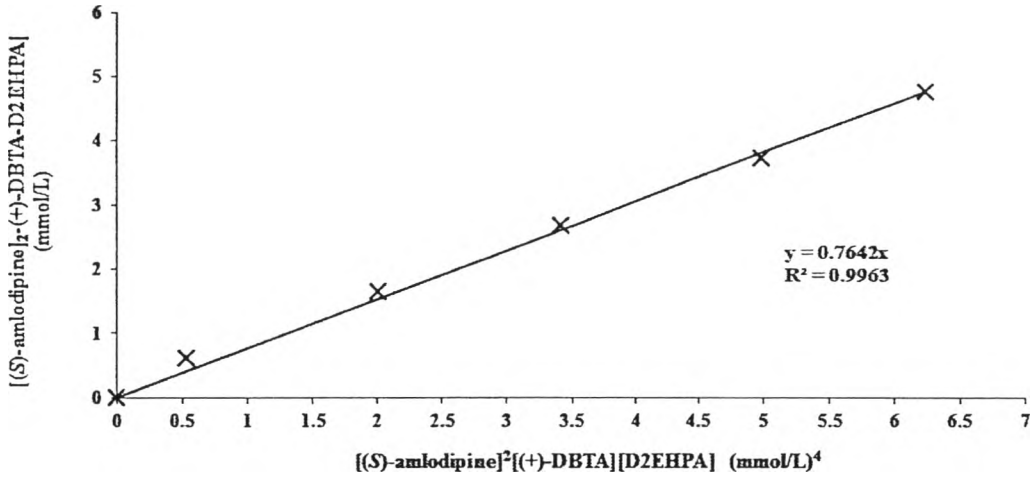

(a)

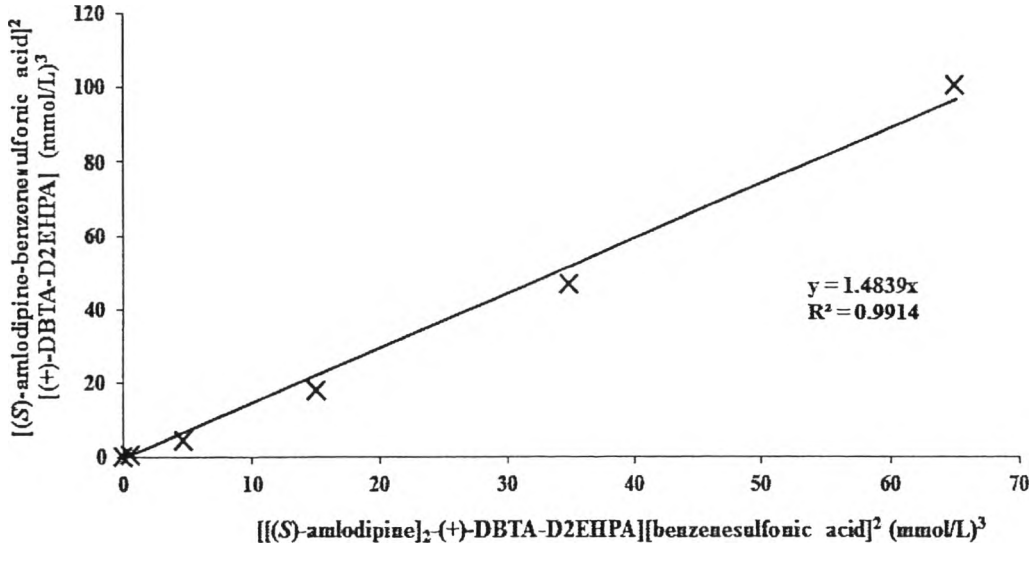

(b)

Figure 4.12 (a) (*S*)-amlodipine extraction with (+)-DBTA-D2EHPA complex as a function of equilibrium [(*S*)-amlodipine]^2[(+)-DBTA][D2EHPA],

(b) (*S*)-amlodipine-(+)-DBTA-D2EHPA stripping with benzenesulfonic acid as a function of equilibrium [[(*S*)-amlodipine]$_2$-(+)-DBTA-D2EHPA] [benzenesulfonic acid]^2

Table 4.3 The distribution ratio (*D*) at the (+)-DBTA concentrations of 2, 4, 6, 8 and 10 mmol/L

[(+)-DBTA] (mmol/L)	2	4	6	8	10
The distribution ration	0.75	2.28	4.34	6.64	9.50

4.5.12 Permeability coefficient

Regarding the permeability coefficient, it could be determined from the expression as proposed by Danesi [54] in Eq. (4.14). The permeability coefficients of (*S*)-amlodipine as a function of concentration of (+)-DBTA from 2 to 8 mmol/L can be obtained from plotting the relationship between $V_f \ln\left(\frac{C_f}{C_{f,0}}\right)$ and time (*t*). $AP\frac{\beta}{\beta+1}$ as the slope is presented in Figure 4.13. And then the permeability coefficients determined from Eq. (4.19) is obtained as shown in Table 4.4.

The results showed that the permeability coefficient increased with the extractant concentration and agreed with the earlier report by Pancharoen *et al.* [66].

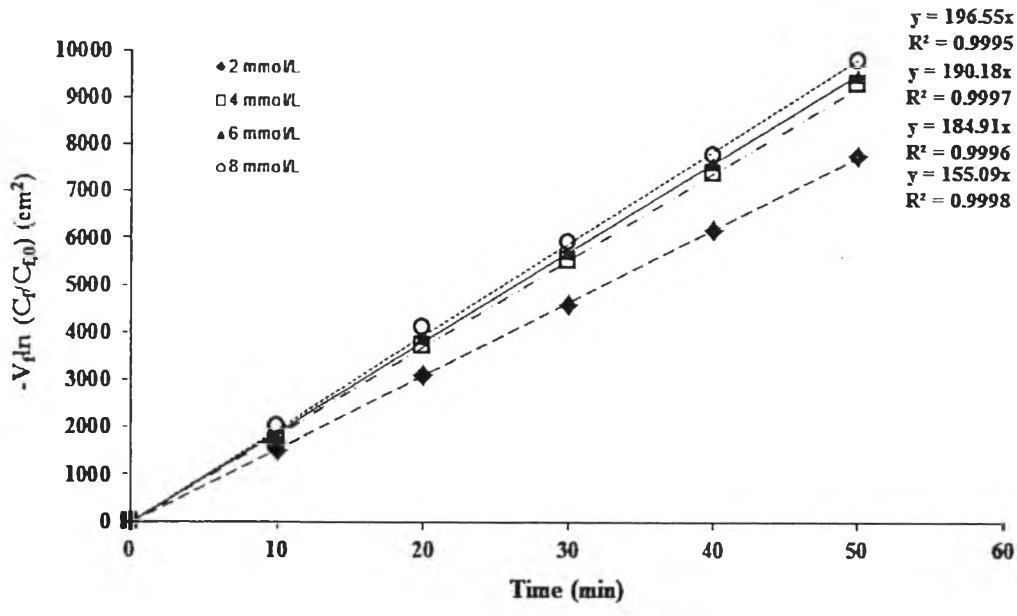

Figure 4.13 The plot of $-V_f \ln (C_f/C_{f,0})$ of (*S*)-amlodipine in feed solution against time with different (+)-DBTA concentrations

Table 4.4 The permeability coefficient (*P*) at (+)-DBTA concentrations of 2, 4, 6 and 8 mmol/L

[(+)-DBTA] (mmol/L)	Permeability coefficients (×100 cm/s)
2	1.75
4	2.34
6	2.46
8	2.62

4.5.13 Mass-transfer coefficients

In Eq. (4.19), mass-transfer coefficient (k_m) of membrane phase and mass-transfer coefficients (k_f) of feed phase were determined by varying the (+)-DBTA concentration. Eq. (4.19) was attained by substituting the membrane-permeability coefficient (P_m) in Eq. (4.18) into Eq. (4.16); assuming that the stripping reaction of (*S*)-amlodipine was instantaneous and there was no contribution of the stripping phase. Eq. (4.19) was used to calculate the aqueous mass-transfer coefficient (k_f) and the membrane mass-transfer coefficient (k_m). By plotting $1/P$ as a function of 1/[(S)-

amlodipine]$_f$ [(+)-DBTA]$_m$ for different carrier concentrations of (+)-DBTA, a straight line with slope $r_i/(r_{lm} \cdot K_{ex} \cdot k_m)$ and ordinate $1/k_f$ for calculation is obtained (Figure 4.14). Thus, the values of k_f and k_m were found to be 4.87×10^{-2} and 2.89×10^{-2} cm/s, respectively. Since the membrane mass-transfer coefficient (k_m) is less than the aqueous feed mass-transfer coefficient (k_f), it can be concluded that the mass transfer across the membrane phase is the mass transfer-controlling step.

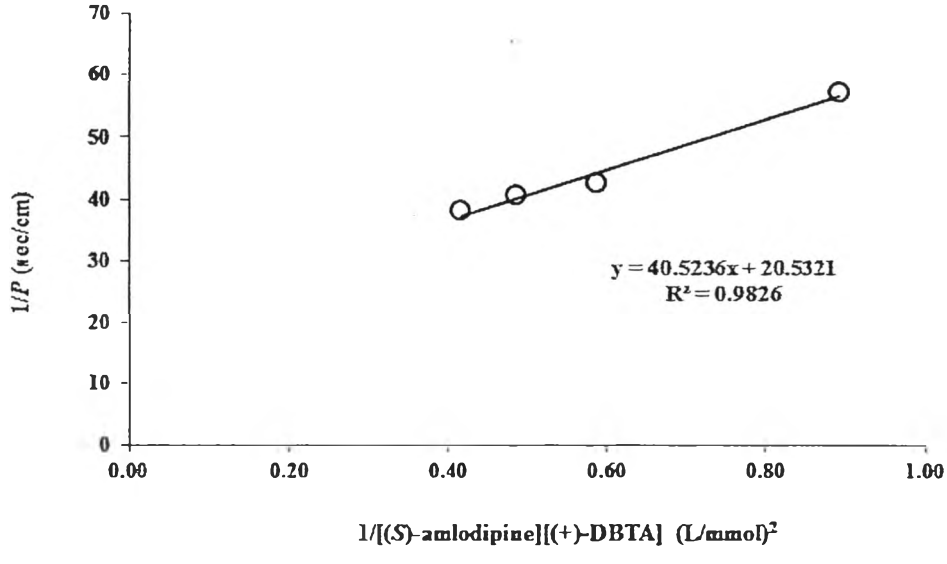

Figure 4.14 The plot of $1/P$ as a function of $1/[(S)\text{-amlodipine}]_f$ $[(+)\text{-DBTA}]_m$

4.6 CONCLUSIONS

This work highlighted that the combination of the extractants cooperated to extract and strip (*S*)-amlodipine from the pharmaceutical industry wastewater by hollow fiber supported liquid membrane. The synergistic effects between (+)-DBTA and D2EHPA could be observed. The high percentages of extraction and stripping were obtained. It is indicated that (*S*)-amlodipine was separated selectively from the racemic mixture of amlodipine by the synergistic extraction of (+)-DBTA with D2EHPA. The (*S*)-amlodipine percentages of extraction and stripping were 84.50% and 80.50%, respectively, from the concentration of synergistic extractant (4 mmol/L (+)-DBTA: 4 mmol/L (+)-D2EHPA), 4 mmol/L benzenesulfonic acid, and 100 ml/min of feed and stripping solutions. The mass-transfer coefficients of the

aqueous phase (k_f) and organic phase (k_m) were 4.87×10^{-2} and 2.89×10^{-2} cm/s, respectively.

This work demonstrates that the synergistic enantioseparation could be selectively extracted (*S*)-amlodipine from racemic amlodipine by using HFSLM. The results demonstrate that the HFSLM with the synergistic-extractant technique was suitable for large-scale production of the pure enantiomeric compound.

4.7 REFERENCES

[1] Thompson, A.M., Hu, T., Eshelbrenner, C.L., Reynolds, K., He, J., Bazzano, L.A. Antihypertensive treatment and secondary prevention of cardiovascular disease events among persons without hypertension: A meta-analysis. JAMA 305(9) (2011): 913-922.

[2] Streel, B., Laine, C., Zimmer, C., Sibenaler, R., Ceccato, A. Enantiomeric determination of amlodipine in human plasma by liquid chromatography coupled to tandem mass spectrometry. J. Biochem. Biophys. Methods 54 (2002): 357-368.

[3] Hardman, J.G., Limbird, L.E. Goodman and Gilman's the pharmacological basis of therapeutics. 10th ed. New Delhi: McGraw Hill, 2001. pp. 853-860.

[4] Yinghua, S., Liang, F., Meng, Z., Wei, L., Ping, M., Li, L., Zhonggui, H. A drug-in-adhesive transdermal patch for *S*-amlodipine free base: In vitro and in vivo characterization. Int. J. Pharm. 382 (2009): 165-171.

[5] Arrowsmith, J.E., Campbell, S.F., Cross, P.E., Stubbs, J.K., Burges, R.A., Gardiner, D.G., Blackburn, K.J. Long-acting dihydropyridine calcium antagonists 1,2-alkoxymethyl derivatives incorporating basic substituents. J. Med. Chem. 29 (1986): 1696-1702.

[6] Goldmann, S., Stoltefuss, J., Born, L. Determination of the absolute configuration of the active amlodipine enantiomer as (-)-*S*: A correction. J. Med. Chem. 35 (1992): 3341-3344.

[7] Park, J.Y., Kim, K.A., Park, P.W., Lee, O.J., Ryu. J.H., Lee, G.H., Ha, M.C., Kim, J.S., Kang, S.W., Lee, K.R. Pharmacokinetic and pharmacodynamic characteristics of a new *S*-amlodipine formulation in healthy Korean male

subjects: a randomized, open-label, two-period, comparative, cross over study. Clin. Ther. 28 (2006): 1837-1847.

[8] Arrowsmith, J.E., Campbell, S.F., Cross, P.E., Stubbs, J.K., Burges, R.A., Gardiner, D.G. Long acting dihydropyridine calcium antagonists. 2. 2-[2-aminoheterocycloethoxy] methyl derivatives. J. Med. Chem. 32 (1986): 562-568.

[9] Lee, H.W., Shin, S.J., Yu, H., Kang, S.K., Yoo, C.L. A novel chiral resolving reagent, bis ((S)-mandelic acid)-3-nitrophthalate, for amlodipine racemate resolution: Scalable synthesis and resolution process. Org. Process Res.Dev. 13 (2009): 1382-1386.

[10] Luksa, J., Josic, D.J., Podobnik, B., Furlan, B., Kremser, M. Semi-preparative chromatographic purification of the enantiomers *S*-(-)-amlodipine and *R*-(+)-amlodipine. J. Chromatogr. B. 693 (1997): 367-375.

[11] Zandkarimi, M., Shafaati, A., and Foroutan, S.M. Chiral separation of basic and zwitterionic drugs by highly sulfated cyclodextrins using short-end injection capillary electrophoresis. Iran. J. pharm. Res. 7(4) (2008): 275-281.

[12] Gotrane, D.M., Deshmukh, R.D., Ranade, P.V., Sonawane, S.P., Bhawal, B.M., Gharpure, M.M., Gurjar, M.K. A novel method for resolution of amlodipine. Org. Process Res.Dev. 13 (2010): 640-643.

[13] Tang, K., Chen, Y.Y., Liu, J.J. Resolution of Zopiclone enantiomers by biphasic recognition chiral extraction. Sep. Purif. Technol. 62 (2008): 681-686.

[14] Maftouh, M., Granier-Loyaux, C., Chavana, E., Marini, J., Pradines, A., Heyden, Y.V., Picard, C. Screening approach for chiral separation of pharmaceuticals: Part III. Supercritical fluid chromatography for analysis and purification in drug discovery. J. Chromatogr. A. 1088 (2005): 67-81.

[15] Lothongkum, A.W., Khemglad, Y., Usomboon, N., Pancharoen, U. Selective recovery of nickel ions from wastewater of stainless steel industry via HFSLM. J. Alloys Compd. 476 (2009): 940-949.

[16] Zhang, W., Cui, C., Ren, Z., Dai, Y., Meng, H. Simultaneous removal and recovery of copper(II) from acidic wastewater by hollow fiber renewal liquid membrane with LIX984N as carrier. Chem. Eng. J. 157 (2010): 230-237.

[17] Kandwal, P., Dixit, S., Mukhopadhyay, S., Mohapatra, P. K. Mass transport modeling of Cs(I) through hollow fiber supported liquid membrane

containing calix-[4]-bis(2,3-naptho)-crown-6 as the mobile carrier. Chem. Eng. J. 174 (2011): 110-116.

[18] Pancharoen, U., Lothongkum, A. W., Chaturabul, S. Mass transfer in hollow fiber supported liquid membrane for As and Hg removal from produced water in upstream petroleum operation in the Gulf of Thailand, in El-Amin, M. (Ed.), Mass Transfer in Multiphase Systems and Its Applications, pp. 499-524. India: InTech, 2011.

[19] Lothongkum, A.W., Panchareon, U., Prapasawat, T. Treatment of heavy metals from industrial wastewaters using hollow fiber supported liquid membrane, in Demadis, K. (Ed.), Water Treatment Processes, pp. 299-332. New York: Nova Science Publishers, 2012.

[20] Lothongkum, A.W., Pancharoen, U., Prapasawat, T. Roles of Facilitated Transport Through HFSLM in Engineering Applications, in Markoš J. (Ed.), Mass Transfer in Chemical Engineering Processes, pp. 177-204. InTech, India, 2011.

[21] Sunsandee, N., Leepipatpiboon, N., Ramakul, P., Pancharoen, U. The selective separation of (*S*)-amlodipine via a hollow fiber supported liquid membrane: modeling and experimental verification. Chem. Eng. J. 180 (2012): 299-308.

[22] Cui, Z. F., Jiang, Y., Field, R.W. Fundamentals of pressure-driven membrane separation processes, in Cui, Z.F. and Muralidhara H.S. (Eds), Membrane Technology: A Practical Guide to Membrane Technology and Applications in Food and Bioprocessing, pp. 12, 16. Elsevier: Butterworth-Heinemann, 2010.

[23] Coelhoso, I.M., Cardoso, M.M., Viegas, R.M.C., Crespo, J.P.S.G. Transport mechanisms and modelling in liquid membrane contactors. Sep. Purif. Technol. 19 (2000): 183-197.

[24] San Roman, M.F., Bringas, E., Ibanez, R., Ortiz, I. Liquid membrane technology: fundamentals and review of its applications. J. Chem. Technol. Biotechnol. 85 (2010): 2-10.

[25] Kocherginsky, N.M., Yang, Q., Seelam, L. Recent advances in supported liquid membrane technology. Sep. Purif. Technol. 53 (2007): 171-177.

[26] Suren, S., Wongsawa, T., Pancharoen, U., Prapasawat, T., Lothongkum, A.W. Uphill transport and mathematical model of Pb(II) from dilute synthetic lead-

containing solutions across hollow fiber supported liquid membrane. Chem. Eng. J. 191 (2012): 503-511.

[27] Lothongkum, A.W., Ramakul, P., Sasomsub, W., Laoharochanapan, S., Pancharoen, U. Enhancement of uranium ion flux by consecutive extraction via hollow fiber supported liquid membrane. J. Taiwan Inst. Chem. Eng. 40 (2009): 518-523.

[28] Rogers, J.D., Long, R. Modeling 686 hollow fiber membrane contactors using film theory, Voronoi tessellations, and facilitation factors for systems with interface reactions. J. Membr. Sci. 134 (1997): 1-17.

[29] Giorno, L., Drioli, E. Enantiospecific membrane processes. Membrane Technol. 106 (1999): 6-11.

[30] Heng, S., Lau, P.P.S., Yeung, K.L., Djafer, M., Schrotter, J.C. Low-temperature ozone treatment for organic template removal from zeolite membrane. J. Membr. Sci. 243 (2004): 69-78.

[31] Heng, S., Yeung, K.L., Djafer, M., Schrotter, J.C. A novel membrane reactor for ozone water treatment. J. Membr. Sci. 289 (2007): 67-75.

[32] Heng, S., Yeung, K.L., Julbe, A.N., Ayral, A.D., Schrotter, J.C. Preparation of composite zeolite membrane separator/contactor for ozone water treatment. Micropor. Mesopor. Mat. 115 (2008): 137-146.

[33] Chan, W.K., Jouët, J.T., Heng, S., Yeung, K.L., Schrotter, J.C. Membrane contactor/separator for an advanced ozone membrane reactor for treatment of recalcitrant organic pollutants in water. J. Solid State Chem. 189 (2012): 96-100.

[34] Prasad, R., Sirkar, K.K. Dispersion-free extraction with microporous hollow fibre modules. AIChE J. 34 (1988): 177-188.

[35] Bortolini1, O., Fantin, G., Fogagnolo, M. Bile acid derivatives as enantiodifferentiating host molecules in inclusion processes. Chirality 17 (2005): 121-130.

[36] Danel, C., Foulon, C., Park, C., Yous, S., Bonte1, J.P., Vaccher, C. Enantiomeric resolution of new aromatase inhibitors by liquid chromatography on cellulose chiral stationary phases. J. Sep. Sci. 28 (2005): 428-434.

[37] Kmecz, I., Simándi, B., Székely, E., Fogassy, E. Resolution of *N*-methylamphetamine enantiomers with tartaric acid derivatives by supercritical fluid extraction. Tetrahedron-Asymmetr. 15 (2004): 1841-1845.

[38] Tang, K.W., Song, L.T., Liu, Y.B., Jiang, X.Y., Pan, C.Y. Separation of flurbiprofen enantiomers by biphasic recognition chiral extraction. Chem. Eng. J. 158 (2010): 411-417.

[39] Tang, K.W., Zhang, P.L., Pan, C.Y., Li, H.J. Equilibrium studies on enantioselective extraction of oxybutynin enantiomers by hydrophilic β-cyclodextrin derivatives, AIChE J. 57 (2011): 3027-3036.

[40] Schuur, B., Winkelman, J.G.M., Heeres, H.J. Equilibrium studies on enantioselective liquid-liquid amino acid extraction using a cinchona alkaloid Extractant. Ind. Eng. Chem. Res. 47 (2008): 10027-10033.

[41] Tang, K.W., Yi, J.M., Liu, Y.B., Jiang, X.Y., Pan, Y. Enantioselective separation of *R,S*-phenylsuccinic acid by biphasic recognition chiral extraction. Chem. Eng. Sci. 64 (2009): 4081-4088.

[42] Kassai, C., Juvancz, Z., Bálint, J., Fogassy, E., Kozma, D. Optical resolution of racemic alcohols via diastereoisomeric supramolecular compound formation with *O,O'*-dibenzoyl-(2*R*,3*R*)-tartaric acid. Tetrahedron 56 (2000): 8355-8359.

[43] Steensma, M., Kuipers, N.J.M. de Haan, A.B., Kwant, G. Identification of enantioselective extractants for chiral separation of amines and amino alcohols. Chirality 18 (2006): 314-328.

[44] Schuur, B., Winkelman, J.G.M., de Vries, J.G., Heeres, H.J. Experimental and modeling studies on the enantio-separation of 3,5-dinitrobenzoyl-(*R*),(*S*)-leucine by continuous liquid-liquid extraction in a cascade of centrifugal contactor separators. Chem. Eng. Sci. 65 (2010): 4682-4690.

[45] Liu, Y.S., Dai, Y.Y., Wang, J.D. Distribution behavior of L-tryptophane by extraction with di(2-ethylhexyl) phosphoric acid. Sep. Sci. Technol. 35 (2000): 1439-1454.

[46] Juang, R.S., Wang, Y.Y. Amino acid separation with D2EHPA by solvent extraction and liquid surfactant membranes. J. Membr. Sci. 207 (2002): 241-252.

[47] Tan, B., Luo, G.S., Qi, X., Wang, J.D. Extractive separation of amino acid enantiomers with co-extractants of tartaric acid derivative and aliquat-336. Sep. Purif. Technol. 53 (2007): 330-336.

[48] Lothongkum, A.W., Suren, S., Chaturabul, S., Thamphiphit, N., Pancharoen, U. Simultaneous removal of arsenic and mercury from natural-gas-co-produced water from the Gulf of Thailand using synergistic extractant via HFSLM. J. Membr. Sci. 369 (2011): 350-358.

[49] Mathur, J.N., Khopkar, P.K. Extraction of trivalent actinides with some substituted pyrazolones and their synergistic mixtures with tri-n-octylphosphine oxide in chloroform. Solvent Extr. Ion Exch. 3 (1984): 1125-1129.

[50] Ramakul, P., Supajaroon, T., Pancharoen, U., Prapasawat, T., Lothongkum, A.W. Synergistic separation of yttrium ions in lanthanide series from rare earths mixture via hollow fiber supported liquid membrane. J. Ind. Eng. Chem. 15 (2009): 224-228.

[51] Tan, B., Luo, G.S., Wang, J.D. Enantioseparation of amino acids by co-extractants with di(2-ethylhexyl)phosphoric acid and tartaric acid derivatives. Tetrahedron-Asymmetr. 17(2006): 883–891.

[52] Luo, F., Li, D., Wei, P. Synergistic extraction of zinc (II) and cadmium (II) with mixtures of primary amine N1923 and neutral organophosphorous derivatives. Hydrometallurgy 73 (2004): 31-40.

[53] Nic, M., Jirat, J., Kosata, B. and Jenkins, A. IUPAC, Compendium of Chemical Terminology, in McNaught, A. D. and Wilkinson. (Eds), The Gold Book 2nd ed. pp. 1-3. Blackwell Scientific Publications, Oxford, 1997.

[54] Danesi, P.R. A simplified model for the coupled transport of metal ions through hollow-fiber supported liquid membranes. J. Membr. Sci. 20 (1984): 231-248.

[55] Pancharoen, U., Wongsawa, T., Lothongkum, A.W. A reaction flux model for extraction of Cu(II) with LIX84I in HFSLM. Sep. Sci. Technol. 46 (2011): 2183-2190.

[56] Chung, Y.S., Ha, M.C. Resolution of the enantiomers of amlodipine. US Patent Application 2003/6646131 B2 (November 11, 2003).

[57] Zandkarimi, M., Shafaati, A., Foroutan, S.M., Lucy, C.A. Rapid enantioseparation of amlodipine by highly sulfated cyclodextrins using short-end injection capillary electrophoresis. DARU 17(4) (2009): 269- 276.

[58] Ramakul, P., Pancharoen, U. Synergistic extraction and separation of mixture of lanthanum and neodymium by hollow supported liquid membrane. Korean J. Chem. Eng. 20 (2003): 724-730.

[59] Ramakul, P., Pattaweekongka, W., Pancharoen, U., Hronec, M. Selective separation of trivalent and tetravalent lanthanide from mixture by hollow fiber supported liquid membrane. J. Chin. Inst. Chem. Eng. 36 (2005): 1-7.

[60] Schultz, G. Separation techniques with supported liquid membranes. Desalination 68 (1988): 191-202.

[61] Ramakul, P., Songkun, E., Pattaweekongka, W., Hronec, M., Pancharoen, U. Permeation study on the hollow-fiber supported liquid membrane for the extraction of cobalts (II). Korean J. Chem. Eng. 23 (1) (2006): 117-123.

[62] Pancharoen, U., Ramakul, P., Patthaveekongka, W. Purely extraction and separation of mixure of cerium(IV) and lanthanum(III) via hollow fiber supported liquid membrane. J. Ind. Eng. Chem. 11(6) (2005): 926- 931.

[63] Tang, K., Song, L., Liu, Y., Miao, J. Enantioselective partitioning of 2-phenylpropionic acid enantiomers in a biphasic recognition chiral extraction system. Chem. Eng. J. 180 (2012): 293-298.

[64] Kazusaki, M., Kawabata H., Matsukura, H. Influence of temperature on enantioseparation employing an amylase-derivative stationary phase. J. Liquid Chromatogr. Relat. Technol. 23 (2000): 2937–2946.

[65] Wannachod, P., Chaturabul, S., Pancharoen, U., Lothongkum, A.W., Patthaveekongka, W. The effective recovery of praseodymium from mixed rare earths via a hollow fiber supported liquid membrane and its mass transfer related. J. Alloy. Compd. 509 (2011): 354-361.

[66] Pancharoen, U., Somboonpanya, S., Chaturabul, S., Lothongkum, A.W. Selective removal of mercury as $HgCl_4^{2-}$ from natural gas well produced water by TOA via HFSLM. J. Alloy Compd. 489 (2010): 72-79.